Near-field microscopy of evanescent microwaves

V. Coello*, R. Villagómez, R. Cortés, and R. López
Centro de Investigación Científica y Educación Superior de Ensenada, Unidad Monterrey, Ángel Martínez Villarreal No. 425, Monterrey, N.L., México 64030

C. Martínez
Doctorado en Ingeniería Física Industrial, FCFM UANL, Av. Pedro de Alba S/N, Edificio de Posgrado, San Nicolás de los Garza, N.L., México 66450

Recibido el 16 de marzo de 2005; aceptado el 27 de junio de 2005

Local control of evanescent microwaves is experimentally investigated using a scanning near-field microwave microscope. The capabilities of the microscope and the contribution, on the near field images, of propagating field components stemming from inelastic (out-of-plane) scattering were elucidated. A set of two-dimensional mirrors for a local control of evanescent modes are shown along with their corresponding near-field image, and their efficiency is discussed. We believe that the experimental approach used is reliable enough to be used as a check of potential (two-dimensional) micro-components and possibly for micro and nano-circuits.

Keywords: Scanning near-field optical microscopy; microwave radiation; wave optics.

El control local de microondas evanescentes es investigado experimentalmente usando un microscopio de barrido de campo cercano en el rango de microondas. Las capacidades del microscopio y la contribución, en las imágenes de campo cercano, de componentes de campo propagativas que proviene de esparcimiento inelástico (fuera del plano) fueron investigadas. Un sistema de espejos bidimensional que sirven para un control local de modos evanescentes es mostrado junto con su correspondiente imagen de cercano-campo y su eficacia es discutida. Nosotros creemos que la aproximación experimental presentada es confiable para ser utilizada como prueba potencial de micro-componentes (de dos dimensiones) y eventualmente para micro y nano-circuitos.

Descriptores: Microscopía óptica de barrido en campo cercano; radiación de microondas; óptica de ondas.

PACS: 61.16.Ch; 84.40.-x; 42.25.-p.

1. Introduction

Evanescent waves occur in different physical phenomena and are suitable for several applications [1]. Studies of evanescent waves can be found in areas such as "forbidden radiation" [1], in surface plasmons polaritons [2], and in the fluorescence of simple molecules near an aperture [3]. A direct probe of evanescent waves is possible using a scanning near field optical microscope (SNOM) [4]. The first SNOM was reported by Pohl and coworkers in 1984 [5], reaching subwavelength optical resolutions close to $\lambda/20$. The success of this kind of imaging system instigated the advent of new configurations [4]. However, for all SNOM versions, the operational principle is found in the detection of *evanescent fields.* Usage of SNOM techniques in the microwave range is an interesting alternative for investigation of subwavelength phenomena since this technique makes "scaling" of the optical problem under question possible. In fact, this type of alternative was used in the first realisation of a high-resolution optical imaging system. The experiment was carried out in the microwave range ($\lambda \approx 3$ cm), reaching a resolution of $\lambda/60$ [6]. This technique has also demonstrated its potential for applications in characterizing magneto-resistivity, superconductivity, and dielectric constant of individual samples [7]. In the same context, resolutions of 100 μm were reached using frequencies in the range of 7.5-12.4 GHz [8] and the inner wire of a coaxial line as the signal probe. There it was established that the resolution of the system was determined by the size of the probe and its distance from the sample. The capability of the Scanning Near-field Microwave Microscope (SNMM) was extended to study sheet resistance from quantitative imaging [9]. The device used has advantages such as measurement of frequency bandwidth, construction from standard commercially available components, and possibilities of improving spatial resolution when using a smaller probe. Even though the mechanical design in the microwave range as well as the precision requirements are not as demanding as in the optical range, SNMMs so far reported are not, or at least to the best of our knowledge, easy to design and operate. In this work, we propose a simple design for SNMM and demonstrate that it works. The SNMM works at a frequency of 10.56 GHz (X-band) and is designed to adopt dissimilar illumination operations modes. We validate our microscope capabilities by presenting studies developed in the microwave scale for potential two-dimensional optics devices.

2. Experimental setup

The experimental setup is schematically depicted in Fig. 1. The setup consists of an SNMM combined with an arrangement for evanescent microwave generation. The evanescent mode is created by means of a coherent microwave beam which is being totally internally reflected inside of a right wax prism ($n \sim$1.43). The prism is mounted onto a metallic round plate that is fixed in a cylindrical base made out of

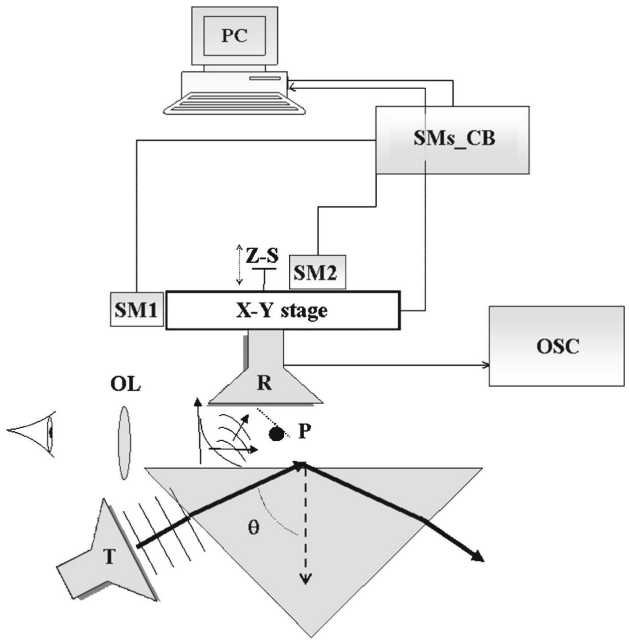

FIGURE 1. Diagram of the scanning near-field microwave microscope for imaging intensity distributions of evanescent modes generated at wavelength λ = 2.85 cm. T, Transmitter; θ, Incidence Angle; OL, Optical Lens; P, Signal Probe; R, Receptor; OSC, Digital Oscilloscope; SMs_CB, Step-Motors Controller Board; PC, Personal Computer; SMI, SM2, Step-Motors 1,2; Z-S, Screw for z-motion.

acrylic material. The microwave source is a commercial unit which consists of a Gunn diode microwave transmitter that provides 15 mW of coherent, linearly polarized microwave output at a wavelength, λ, of 2.85 cm. The whole unit is composed of the Gunn diode located in a 10.525 GHz resonator cavity, a microwave horn to direct the output, and an 18 cm stand to help reduce table top reflections. The Gunn diode acts as a non-linear resistor that oscillates in the microwave band. The output is linearly polarized along the long axis of the Gunn Transmitter diode (*i.e.*, as the radiation propagates through space, its electric field remains aligned with the long axis of the diode). The microwave receiver is a microwave horn, identical to that of the transmitter, that collects the signal and channels it to a Schottky diode in a 10.525 Ghz resonant cavity. The diode responds only to the component of a microwave signal that is polarized *along* the diode axis, producing a DC voltage that varies with the magnitude of the microwave signal. The scanning of the microscope is carried out using a non-commercial stand-alone type scanner *i.e.*, the probe is scanned along a fixed sample. The advantage of the stand alone scanner is that it can easily be used to scan different parts of large samples while keeping the illumination configuration unchanged. The scanner is particularly simple in design and it is based on a system of two steps motors for motion control in the *xy* plane. The scanner motion is computer controlled via a non-commercial motor control card. The probe used for the experiments is a metallic (iron) sphere with a radius of $\sim$ 3mm. The probe acts as a scatterer of the evanescent field, leading to homogeneous waves which can be easily detected. The distance between the surface and the probe was set by using a micrometer translation stage. Once the probe is brought near the surface, the maximum level in the detected signal is taken as the probe-sample contact point. A magnifying lens is used for visual inspection of the probe-to-sample distance control. The mapping of the signal is carried out in a constant height mode. As the raster-scan drags the probe over the sample, the very end of it slightly touches the surface generating friction forces between the tip and the sample. In order to reduce the drag effect friction forces, the probe has been placed at the end of a leaf spring or "cantilever" that is made out of acrylic material. Consequently, once the probe is in surface contact, the cantilever suffers a vertical deflection which allows the device to scan over local sample heights up to $\lambda/2$ order of size. Finally, the signal is sent to a digital oscilloscope [10]. The signal is collected and digitally processed by our non-commercial computer software which code provides $x - y$ probe positioning capability and scan speed control. The speed of the scan is basically limited by the number of collected data in every single mapped point. Typical collected values number 5000, ensuring a sufficiently high signal-to-noise ratio in the detected signal. The resolution of the step motors has been fixed at 0.125 cm for every single step or equivalent image element (pixel).

3. Results and discussion

First, the capability of the microscope for mapping an evanescent mode was elucidated. Thus, we imaged a standing evanescent wave pattern that was created by directing the microwave beam perpendicular to a side face of a 90°wax prism, thereby obtaining the interference pattern related to the counter-propagating totally internally reflected waves with different amplitudes. In order to show its evanescent

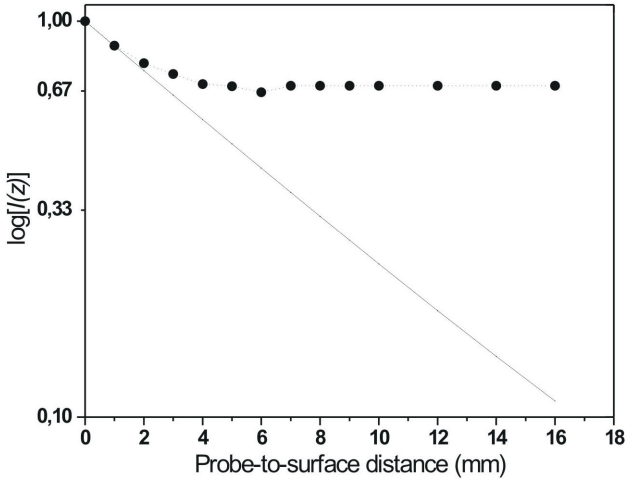

FIGURE 2. Calculated (solid line) and measured probe-to-surface distance dependence of the signal for the wax prism. Dashed line connecting the experimental points serve to guide the eye.

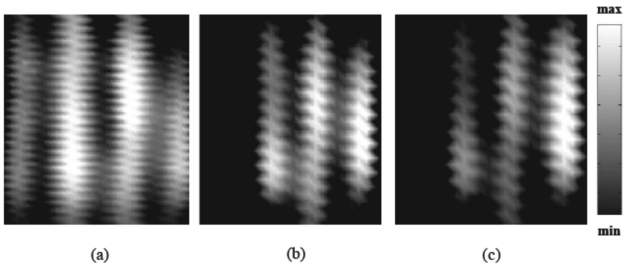

FIGURE 3. Gray-scale near-field images of 4 x 4 cm^2 generated due to the standing evanescent wave at the surface on the base of the wax prism. The images were taken at the same place for different probe-to-surface distances: ∼0 (a), 2 (b), and ∼10 mm (c).

nature, an experimental study of the probe-to-sample distance dependence of the signal was carried out. For small distances, such dependence exhibited the expected exponential decay with the increase of the distance. The average signal decreased about three times for a distance around 5 mm from the surface, and was then practically independent of the tip-surface distance (Fig. 2). Consequently, the interference pattern of the evanescent waves was visible only up to a probe to-surface distance of ∼5 mm (Figs. 3a-3c). A high-frequency oscillation perpendicular to the direction of propagation (Figs. 3a-3c) was also observed. The oscillation is supposed to be stem from the electronic noise and/or mechanical vibrations of the scanner. Typically, those image artifacts appear as oscillations or repeating patterns in the image and they can be amended digitally *a posteriori* by using image processing.

Concerning the local (in-plane) control of evanescent microwaves, a single circular nano-particle scatterer is an adequate choice in order to maximize the scatterer's strength while preserving an adiabatic perturbation [11,12 and references therein].

In this context, we characterized individual iron-spheres (Figs. 4a-4f) in order to determine the radius size which would respond more efficiently to the desirable effect of elastic scattering of evanescent microwaves mode. The metallic sphere is fixed at the wax surface by means of conduction local heating of the surface. The process is developed by pressing the sphere against the wax surface with the very end of a sharpened warm metal wire. Therefore, the desirable point in the surface is melted but the whole prism is only slightly warmed, to prevent damaging of it. This results in a simple and reliable technique for placing individual spheres and therefore for creating any kind of conceivable components. We found that a sphere of radius ∼ 1.5 cm (Fig. 4d) produced a perturbation of the signal in the form of nearly parabolic interference fringes (Fig. 4c). The effect is similar to that reported for the optical case [12]. The perturbation of the signal is better visualized when comparing images with (Fig. 4c) and without (Fig. 4a) sphere. Once the size of the sphere is increased to about double (Fig. 4f), the elastic scattering is not longer preserved, and the picture becomes complicated due to the inelastic (out of the plane) scattering (Fig. 4e). By placing scatterers in line arrays, a common plane wavefront of the scattered light can be achieved. From an application point of view, it is very promising to exploit line arrays to reflect the wavefront of the applied field to make a mirror effect. The idea has been carried out for a 5-scatterer line array, whose inclination with respect to the applied field is 90° and with inter-particle distances equal to $\lambda/2$. The image for the line mirror showed the interference between a specular reflected evanescent microwave and the incident one, exhibiting a satisfactory behaviour of the line mirror for normal incidence (Figs. 5a, 5b). Another two-dimensional component realizable by a certain array structure of scatterers is a focusing mirror (Figs. 6a-6c). Ideally the focusing mirror should consist of scatterers placed along a parabolic curve $(y - y_0)^2 = 4F(x - x_0)^2$, where (x, y) is the orthogonal system of coordinates in the surface plane, the coordinate (x_0, y_0) is located at the bottom of the mirror, and F is the focal length. The x axis is oriented along the optical axis. Based on that, we fabricated a mirror with F= 2.5 cm. It is seen that we did not fail to align 7 microscatterers along a curved line, and the expected focusing was clearly exhibited (Fig. 6 (a)). Such an effect was even more clearly seen in the enhancement up to oven 10 times that of the recorded intensity distributions in the focusing region (Fig. 6c). Taking into account the fact that the signal in the focusing region is enhanced several orders of magnitude, one can assume that this effect is indeed an exciting feature related to the fabricated microcomponent. Two dimensional focusing micromirrors are very interesting in the sense that they offer the possibility of enhancing the signal locally in a controllable way. For instance, this feature could be exploited, possibly in connection with a focused excitation

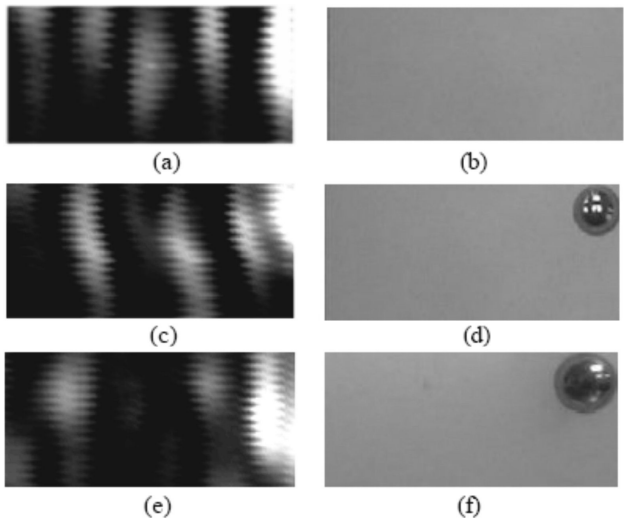

FIGURE 4. Gray-scale near-field images of 4 x 8 cm^2 due to the elasti scattering of an evanescent microwave mode travelling from left to right on the wax surface prism (a,c,e), and corresponding surface digital picture showing a sphere of radius of 0 (b), 1.5 (d) and 3 (f) cm. Scale bar for near field images is the same as in Fig. 3.

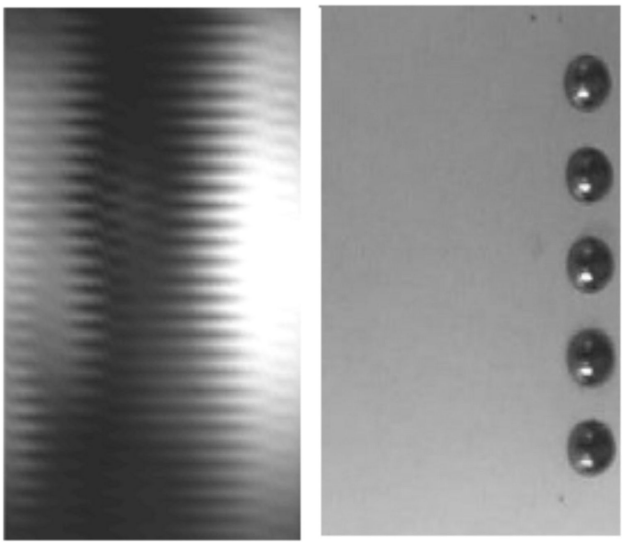

(a) (b)

FIGURE 5. Gray-scale near-field image of 4.5×10 cm^2 due to the elastic scattering of an evanescent microwave mode travelling from left to right on the line of scatterers placed along the wax surface prism (a), and corresponding surface digital picture. Scale bar for the near field image is the same as in Fig. 3.

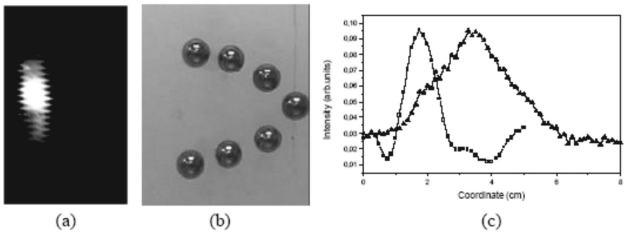

(a) (b) (c)

FIGURE 6. Gray-scale near-field image of 4×6 cm^2 due to the elastic scattering of an evanescent microwave mode travelling from left to right on the parabolic line of scatterers placed along the wax surface prism (a), and corresponding surface digital picture (not to scale) (b). In (c), squares and triangles are horizontal and vertical cross sections respectively of (a). The horizontal cross section is along the optical axis of the parabolic line, and the vertical one is across the focusing area. Solid lines connecting the experimental points serve to guide the eye. Scale bar for the near field image is the same as in Fig. 3.

source, to further increase the efficiency of surface enhanced Raman spectroscopy.

4. Conclusions

We have designed and constructed a stand-alone SNMM, including electronics and software, and demonstrated that it works. The SNMM showed capabilities for imaging of evanescent microwaves. The nature of the detected signal was confirmed by sample-to-probe distance dependent on a generated standing wave interference pattern. The observed oscillation perpendicular to the direction of propagation may have its origin in electronic noise and/or mechanical vibrations of the scanner. Two kind of potential two-dimensional optical mirrors were artificially fabricated by simply aligning metal spheres that have been placed above the wax prism surface. The line mirror observed the reflection laws, and Wiener fringes were already exhibited. The experiment also showed a line mirror behaviour that was not as perfect as expected. For example, the line mirror did not completely backward reflect the incident evanescent mode, and showed transmission. We believe that this phenomenon can be compensated for by making use of the photonic band gap effect, *i.e.*: by placing additional lines parallel to the first with separation distances that satisfy the Bragg condition, $2d \sin\theta$, where d is the separation distance, θ is the angle the incident field makes with the mirror, and n is a whole number. The focusing effect of the parabolic mirror showed an enhancement of the signal up to 10 times the background, indicating that this fabrication technique can be used, with certain limitations, as a check for testing potential micro and nano components assembled of individual scatterers, *e.g.*, beam-splitters and interferometers [13,14]. We are conducting further investigations in this area.

∗ correspondence author: e-mail: vcoello@cicese.mx

1. F. de Fornel, *Evanescent Waves: from Newtonian Optics to Atomic Optics Springer series in optical science* (Springer, Berlin, 2001).

2. H. Raether, *Surface Plasmons, Springer Tracts in Modern Physics* (Springer, Berlin, 1988) Vol. 111; *Surface Polaritons*, edited by V.M. Agranovich and D.L. Mills (North-Holland, Amsterdam, 1982).

3. B. Valeur, *Molecular Fluorescence: Principles and Applications* (John Wiley and Sons 2002).

4. *Near Field Optics*, edited by D.W. Pohl and D. Courjon (Kluwer, The Netherlands, 1993); D Courjon and C Bainier, *Rep. Prog. Phys.* **57** (1994) 989.

5. D.W. Phol, W. Denk, and M. Lanz, *Appl. Phys. Lett.* **44** (1984) 651.

6. E. Ash and G. Nicholls, *Nature* **237** (1972) 510.

7. T. Wei, X.-D. Xiang, W.G. Wallace-Freedman, and P.G. Schultz, *Appl. Phys. Lett.* **68** (1996) 24.

8. C.P. Vlahacos, R.C. Black, S.M. Anlage, A. Amar, and F.C. Wellstood, *Appl. Phys. Lett.* **69** (1996) 21.

9. D.E. Steinhauer *et al.*, *Appl. Phys. Lett.* **72** (1997) 7.
10. Tektronik, Digital Phosphor Oscilloscope, TDS3000B Series.
11. V. Coello, S.I. Bozhevolnyi, and F.A. Pudonin, *Proc. SPIE* **3098** (1997) 536.
12. S.I. Bozhevolnyi and V. Coello, *Phys. Rev. B.* **58** (1998) 10899.
13. H. Dittlbacher, J.R. Krenn, G. Shider, A. Leitner, and F.R. Aussenegg, *Appl. Phys. Lett.* **81** (2002) 1762.
14. V. Coello, T. Søndergaard, and S.I. Bozhevolnyi, *Opt. Comm.* **240** (2004) 345.